An implantable PDMS tool for heightened throughput in screening hMSC differentiation potential *in vivo*

Q. Vallmajo-Martin[1,2], I. Martin[3], M. Lütolf[2], M. Ehrbar[1]

[1] Laboratory for Cell and Tissue Engineering, University Hospital Zürich, Switzerland, [2] Laboratory of Stem Cell Bioengineering, EPFL Lausanne, Switzerland, [3]Department of Biomedicine, University Hospital Basel, Switzerland

INTRODUCTION: Clinical translation of tissue engineering approaches for healing traumatic bone injuries necessitates a robust method to evaluate the cell sources and growth factors that are critical for osteogenesis.

METHODS: To address this, we designed a polydimethylsulfoxane (PDMS)-based implantable tool to decipher the individual contributions of different human cell sources and/or growth factors to bone formation. Each PDMS tool contains separated wells for different conditions to be screened in parallel and can be implanted subcutaneously in mice allowing for up to 32 unique conditions to be evaluated per animal. In each well, individual polyethylene glycol (PEG) hydrogels (PEG was selected as a defined non-inductive 3D environment) were seeded with various combinations of human mesenchymal stem cells (hMSCs) from diverse sources and bone morphogenetic protein-2 (BMP-2).

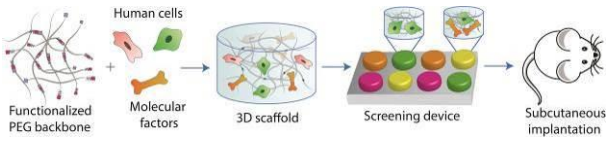

Fig.1: In vivo niche screening device. Modular PEG hydrogels, growth factors and cells are employed to create microenvironments of variable composition in the 4x 8-well screening devices that are subcutaneously implanted per mouse.

RESULTS: We first determined the minimum concentration of BMP-2 and minimum cell density for bone marrow-derived hMSCs from healthy donors. Strikingly, we found that hMSCs without presence of BMP-2 could remodel PEG gels into ossicles after 8 weeks in vivo. MicroCT analysis showed presence of mineralization within the constructs, a characteristic further corroborated by histology. Moreover, these implants not only still contained hMSCs, but were also highly infiltrated by murine osteogenic, endothelial and hematopoietic cells as demonstrated by FACS analysis and histological stainings. When different hMSC sources were compared in this system, it was found that adipose-derived, as well as bone marrow derived hMSCs from osteoporic patients, failed to mineralize in vivo.

DISCUSSION & CONCLUSIONS: Results indicated that at a high cell density, bone marrow-derived hMSCs alone can induce bone formation in an inert environment without any inductive factors. Importantly, tissue type and donor health significantly affect hMSC potential. This shows that we have developed a robust system to systematically determine these differences. The PDMS screening device is a powerful new tool for heightened *in vivo* screening of tissue engineering constructs with a broad range of applications.

ACKNOWLEDGEMENTS: This work was funded by the Swiss National Science Foundation grant 153316.

Three-dimensional cardiac tissue generated via a scaffold-free oxime ligation method

D. Rogozhnikov[1,2], P. O'Brian[1], S. Elahipanah[1], M. Yousaf[1]

[1] Department of Chemistry, York University, Toronto, Canada. [2]Laboratory of Tissue Engineering and Biofabrication, Department of Health Sciences and Technology School of Biosciences, ETH Zurich, Switzerland

INTRODUCTION: The generation of complex three-dimensional (3D) tissues with multiple cell types in vitro is a major goal of lab on a chip research but also includes tissue engineering and artificial organ research fields. Cardiovascular associated diseases are the leading cause of death globally and account for 30% of deaths worldwide. Production of 3-dimensional artificial cardiac tissues for both transplantation and evaluation of drug toxicity has been an intense area of research. Herein, we present a scaffold-free method to generate 3-dimensional cardiac tissue. The strategy combines cell surface engineering and bio-orthogonal chemistry to rapidly assemble 3 different cell types to generate a functional cardiac tissue. This is the first example of a 3-dimensional cardiac tissue that does not consist of an external supporting scaffold. The resulting tissue was used to evaluate drug toxicity.

METHODS: Cardiomyocytes, cardiac fibroblasts and HUVECs were used to construct cardiac tissues. Harvested cells were treated with ketone or oxyamine-containing liposomes. The liposome fusion process occurs in seconds to minutes and installs the bio-orthogonal groups onto the cell surface. It should be noted that the liposome fusion/bio-orthogonal delivery technology works on many mammalian cell types and is fast, mild and operates within seconds to tailor cell surfaces on freshly harvested cardiomyocytes from rat hearts. The 3 surface-engineered cell types were mixed and rapidly assembled into 3D tissues.

RESULTS: Cardiac cells were assembled into 3D tissues. The thickness of tissues which resulted from assembly of cells treated with

oxyamine or ketone-functionalized liposomes was measured to be ~50 µm (*Fig.1*) The cells that were not treated with liposomes could only produce thin monolayers with thickness of only 12µm. The 3D cardiac tissues were further characterized for the expression of cardiac-specific markers: cTnT and Cx 43 as well as for collagen secretion. Finally, the engineered 3D cardiac tissues were used to assess the cardiotoxic effect of two chronotropic drugs: isoprenaline and doxorubicin.

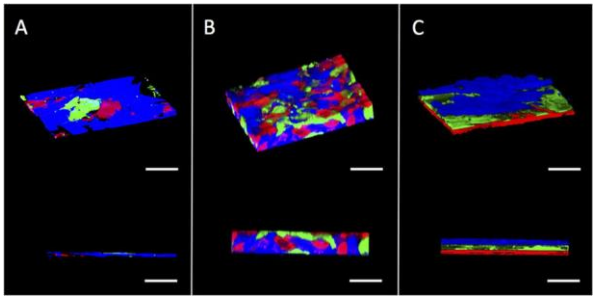

Fig. 1: Confocal image representations of 2D and 3D scaffold free cardiac tissues. Scale bar = 60 µm

DISCUSSION & CONCLUSIONS: Herein we utilized bio-orthogonal oxime click chemistry to assemble cells into functional 3D cardiac tissues without the use of scaffold materials. The tissues were utilized for drug screening purposes. We believe the combination of liposome fusion, bio-orthogonal chemistry and cell surface engineering will have a significant impact on autocrine and paracrine signalling studies and for the development and evaluation therapeutic organ on a chip based biotechnology applications.

ACKNOWLEDGEMENTS: This work was supported by National Science and Engineering Research Council (NSERC) of Canada.

Biomimetic cartilage/ bone interface

W. Baumgartner[1], L. Otto[1], S.C. Hess[2], W.J. Stark[2], S. Märsmann[1,3], G. Meier Bürgisser[1], M. Calcagni[1], P. Cinelli[3], J. Buschmann[1]

[1] Plastic Surgery and Hand Surgery, University Hospital Zurich, Zurich Switzerland.
[2]Institute for Chemical and Bioengineering, ETH Zurich, Zurich Switzerland. [3] 3Division of Trauma Surgery, University Hospital Zurich, Zurich Switzerland.

INTRODUCTION: The interface between cartilage and bone is characterized by a gradient of calcium phosphate phases that decline in content from bone towards cartilage. Adipose-derived stem cells are able to differentiate into chondrocytes and osteoblasts, offering the option to use one single cell source for tissue engineering of a biomimetic cartilage/ bone interface.

METHODS: We used an electrospun poly-lactic-co-glycolic acid (PLGA) mesh with incorporated amorphous calcium phosphate nanoparticles in different weight percentages, having a gradient from 30%, 20%, 10% and 0% towards the cartilage mimicking side of the biomimetic interface. The materials were seeded with human adipose-derived stem cells (ASCs) and either cultivated under static conditions or under dynamic conditions in a perfusion bioreactor without any further supplementation of the culture medium. After a total of four weeks, quantitative RT-PCR was performed for eleven relevant genes, including typical marker genes for osteo- and chondrogenesis, but also for adipo- and angiogenesis. In addition, histology and immunohistochemistry was performed to address cell density and glycosaminoglycans.

RESULTS: Under static conditions, the presence of amorphous calcium phosphate nanoparticles did not have any impact on osteo- and chondrogenesis related genes – only CD31 (and endothelial marker gene) was upregulated in the presence of nanoparticles compared to pure PLGA. In contrast, under dynamic conditions, ASCs exhibited an increased expression of chondrogenic marker gene Sox9 towards the cartilage mimicking side. In addition, ASCs showed an increased expression of osteogenic marker gene osteocalcin towards the bone mimicking side. The results found on the gene level were supported by findings on the protein level.

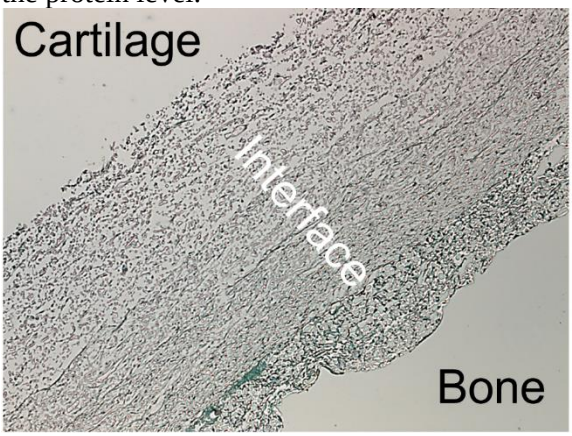

Fig. 1: Osteochondral interface. Safranin O stained histological cross-section through the eight layers of the piled 3D construct.

DISCUSSION & CONCLUSIONS: We conclude that amorphous calcium phosphate nanoparticles incorporated in electrospun PLGA meshes influence the differentiation behaviour of human ASCs. Electrospun meshes with gradients of nanoparticles may act as promising cartilage/bone interfaces when cultivated under perfusion in a bioreactor system.

ACKNOWLEDGEMENTS: We thank Andrea Garcete-Bärtschi and Ines Kleiber-Schaaf for Sox9, Alcian Blue and Safranin O stainings.

Flexible reinforced hydrogels

E. Tosoratti[*1], J. Beaudin[*2], M. Zenobi-Wong[1], C. Leinenbach[3]
[1]Tissue Engineering + Biofabrication, ETH, Zürich, CH. [2]Department of Bioengineering, Imperial College London, [3]Advanced Materials Processing, Empa, Dübendorf, CH

INTRODUCTION: Nowadays, most bio-fabrication approaches are based on the use of cells and biopolymers such as hydrogels. While this method ensures a biocompatible environment for cells, the overall mechanical properties of the grafts are too weak to maintain their shape for long periods of time in vivo. A novel class of hybrid reinforced grafts using titanium is developed in order to provide soft tissue implants with additional mechanical stability and flexibility.

METHODS: Structures with flexible properties are designed in Fusion 360. Different unit cells are patterned in 2D to form plates which are connected one to another by flexible arms. Computational analysis is performed using Abaqus CAE on different unit cells and connecting arms shapes to assess the constructs' behaviour under physiological environments. Samples are 3D printed using Titanium Ti-6Al-7Nb powder using a Sisma mysint100. Different concentrations of alginate (1%, 1.5% and 2%) were combined with the reinforcement material and crosslinked using 100mM $CaCl_2$. Compression tests were performed using a Ta.XT plus Texture analyser (stable micro systems). 15% strain was applied to the samples consistently.

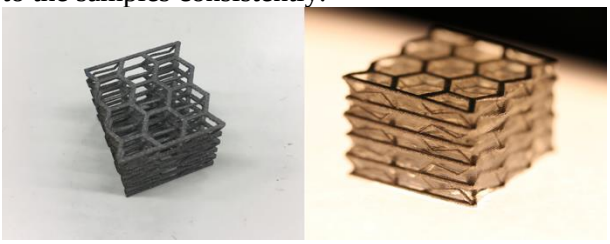

Fig. 1: (A) 3D Metal Printed sample. (B) 3D printed PLA sample. (C+D) samples backfilled with alginate hydrogel.

RESULTS: Figure 1 shows the 3D metal printed constructs before and after being backfilled with alginate. The 3D printed metal scaffolds and alginate hydrogels have shown good interface adherence and Young's Modulus in the range of 350-700 kPa. Figure 2 shows the compression curves for a hexagonal unit cell. A hydrogel's compression characteristic curve is observed in combination with the titanium's compressive strength.

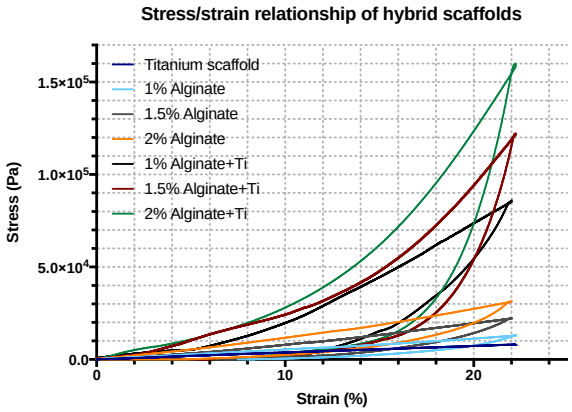

Fig. 2: Stress strain curves for different alginate concentrations + Ti scaffold.

DISCUSSION & CONCLUSIONS: The Ti reinforcement design allows to generate structures with flexible properties at specific locations. The integration of the alginate hydrogel adds energy absorption properties useful in many physiological applications. This tunability allows the design of structures which mimic natural organs allowing to enhance flexibility or increasing strength at precise locations.

Delamination of the hydroxyapatite coating from the stem 14 months after total hip arthroplasty – A case report

P. Wahl[1], C. Meier[1], A. Dommann[3], A. Neels[3], C.M. Sprecher[2]

[1] Cantonal Hospital Winterthur, CH, [2] AO Research Institute Davos, CH
[3] EMPA Swiss Federal Laboratories for Material Science and Technology, St.Gallen, CH

INTRODUCTION: Hydroxyapatite (HA) coating has become very popular in uncemented total hip arthroplasty (THA).[1] The surface topography of this coating, with increased porosity compared to roughened titanium, might help accelerate integration of the implant by the surrounding bone.[2,3] But the interface between such a coating and the underlying metal represents by definition a potential rupture point, as the mechanical properties of both materials differ. We present a case where it could be documented that the HA coating separated from the stem and this contributed to early failure after THA.

CASE REPORT: Uncemented THA with an HA coated stem had been performed elsewhere 14 months earlier in a 68 years old deaf and dumb male patient to treat a femoral neck fracture associated with osteoporosis. A minor trauma induced a comminuted periprosthetic fracture, which required an exchange of the completely loose stem. The stem could be recovered without any instrumentation and a new implant was set. Early recovery and rehabilitation up to now 4 months postoperatively are uneventful.

METHODS: Radiologic studies are presented. The structure of the implants surface was photo documented. Tissue specimens sampled during debridement of the medullary cavity of the proximal femur have been examined by μCT. The crystallographic phases of the HA coating were determined by x-ray diffraction (XRD) methods.

RESULTS: Conventional radiographies identified a thin and dense line parallel to the medial edge of the implant. Analysing by uCT of the corresponding tissue samples identified this to be the HA coating of the stem, which had been well integrated by bone, but showed a full-thickness separation from the implant. Only HA as crystallographic phase could be detected on bone or implant side of the coating. Material chipped of the coating however identified alterations of the structure of the HA. Local polishing of the roughened surface of the stem was also identified.

DISCUSSION & CONCLUSIONS: Undersizing of the stem at primary uncemented THA in an osteoporotic bone not only contributed to the fracture,[4] but also provided an exceptionally rare occasion to analyse materials otherwise not available to sampling. This confirmed good bone ongrowth on the HA layer, but the coating had separated entirely from the underlying metal of the stem. Partial polishing of the sandblasted surface of the metal of the stem indicates separation of the HA coating long before the trauma. Energy from this trauma should have been insufficient for that. Failure of the interface between the metal of the stem and the HA coating after only 14 months in situ is a poor result for a permanent implant. HA being much harder than the stems titanium alloy, micromovements of the stem could thus lead to abrasion of its surface. Any residues of the HA coating also had to be removed before reconstruction with a new stem to prevent residual HA layers to act as a barrier and hinder bone ongrowth,. XRD revealed the presence of crystalline HA in the coating of the stem retrieved after 14 months. Closer investigation of the interface between the Ti-Alloy and the HA phase showed no additional crystalline phases are present. However, the analysis of the powdered material chipped off the metal showed the presence of smaller crystallites and nano-sized (<100 nm) particles compared to the HA powder obtained from new implants. This however needs further investigations on similar cases as the behaviour of HA coatings in situ remains largely unknown. Further analysis needs to be performed, also on other retrievals from early failed THA, to determine if the problem identified is a single case, if it is associated with a specific brand or if it can be identified throughout various models of HA coated stems. Cases allowing adequate sampling however remain rare.

Transdermal application of curcumin to treat bacterial infection in a 3D skin model

B. Senturk[1], C. Fessele[1], B. von Rechenberg[2], F. Hahn[3], M. Rottmar[1]

[1]Biointerfaces, Empa, Swiss Federal Laboratories for Materials Science and Technology, St.Gallen, CH. [2]MSRU, Vetsuisse Faculty ZH, University of Zurich, CH. [3]MedDrop Technology AG, Zurich, CH

INTRODUCTION: Due to a serious increase in the number of patients suffering from diabetes and obesity worldwide, the prevalence of chronic skin wounds is on the rise.
However, current treatments such as wound dressings, hydrogels and drugs for chronic wounds fail to achieve effective therapeutic outcomes. A new therapeutic approach for treating deep, chronic and non-healing wounds efficiently and without pain for the patient is urgently needed. Active pharmaceuticals have great promise, and should ideally have both anti-microbial and wound healing-promoting properties, as well as potential for easy and extensive topical application in clinical settings.
In this work, the anti-microbial and anti-inflammatory properties of different active pharmaceutical ingredients (API), intended to promote wound healing via transdermal application (TDA), was investigated in vitro.

METHODS: Cell viability, cell migration and cell proliferation were investigated by AlamarBlue assay, wound scratch assay and BrdU proliferation assay, respectively. Anti-inflammatory effect of curcumin was examined by RT-PCR analysis of pro-inflammatory markers (CD197, CXCL10) on THP1 cells treated with LPS. Secretion of inflammatory cytokines TNF-α, IL-6 and IL-8 were measured by ELISAs. Fibroblast to myofibroblast differentiation was assessed by α-SMA staining of NHDF cells and visualized by confocal laser scanning microscopy. The antibacterial and anti-biofilm activity of the API formulations were tested on *S. aureus* and *P. aeruginosa*.
A 3D full thickness skin model, encompassing a dermal and an epidermal compartment consisting of primary human fibroblasts, and primary human keratinocytes differentiated with air-lift culture was established. The 3D skin model is used to study skin infection and to evaluate the effects of API. One API, curcumin, was applied to the infected area of the skin using TDA technology and its effect was evaluated by histological analyses.

RESULTS: From 15 different API, most promising results were obtained with curcumin treatment. RT-PCR analysis showed that expression of pro-inflammatory marker CD197 and CXCL10 was significantly reduced in curcumin treated THP-1 cells (Figure1). Notably, with increasing curcumin concentration, cell viability decreased while the anti-inflammatory effect increased. However, HDF, HEK and THP-1 cells treated with 20 µM of curcumin did not show any toxicity. Furthermore, curcumin treatment had an anti-bacterial effect on S.aureus, but was not efficient on *P. aeruginosa*.

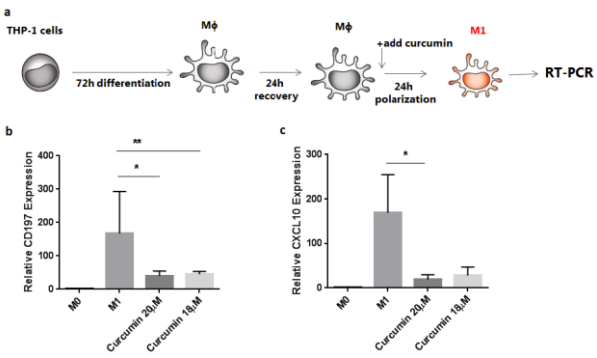

*Fig. 1: Anti-inflammatory activity of curcumin treatment. a) Schematic representation of the experiment with curcumin being added after differentiation of THP-1 cells with PMA treatment. CD197 (b) and CXCL10 (c) gene expression analysis of curcumin treated macrophages. Expression levels ±SD of each gene were normalized to M0. GAPDH was used as housekeeping gene. n=3 (**p< 0.01, *p< 0.05).*

DISCUSSION & CONCLUSIONS: Curcumin treatment shows both anti-inflammatory and anti-bacterial activity. These results indicate that curcumin treatment via transdermal application can be used to support the impaired healing process in chronic wounds.**CKNOWLEDGEMENTS:** This work is supported by CTI-PFLS 18524.2 project

Biodegradable and bone targeting drug delivery system for antibiotics

S.G. Rotman[1,2], D.W. Grijpma[2], R.G. Richards[1], T.F. Moriarty[1], D. Eglin[1] and O. Guillaume[1]

[1]AO Research Institute, AO Foundation, Davos, CH. [2] Department of Biomaterials Science and Technology, University of Twente, The Netherlands

INTRODUCTION: Bone infection is a serious complication with high (up to 30%) incidence in open bone fractures[1]. Current treatment strategies involve a debridement of the infected tissue, followed by a combined therapy with systemic antibiotics and the implantation of antibiotic releasing biomaterials. The success rate of such therapies is still insufficient, with 30% of the patients showing recurrence of the infection after 12 months. The impaired blood supply to the tissue surrounding the infection prevents optimal supply of systemic antibiotics, and many antibiotic loaded biomaterials show either too fast or insufficient drug release. In this work, we propose a local bone targeting drug delivery system for antibiotics to treat recurrent bone infection.

METHODS: 10 w/v% PCL (M_w = 80.000 g·mol^{-1}, PDI = <2) or 10 w/v% PLA (M_w = 215.000 g·mol^{-1}) and 2.5 wt% antibiotic (Rifampicin (RIF) or Gentamicin-AOT (Gen-AOT)) were dissolved in dichloromethane. The polymer/drug solutions were emulsified in a 1 w/v% PVA (M_w = 31.000 g·mol^{-1} Carl Roth, Switzerland) solution in water using sonication probe or an ultra turrax. The PCL particles were collected after washing to remove surfactant. The particles were dispersed in 0.1M NaOH solution for saponification of the PCL particle surface. EDC/NHS conjugation allowed covalent binding of the Alendronate (ALN) with the PCL microparticle. Antibiotic release profiles were measured in phosphatase saline buffer (PBS) using high performance liquid chromatography (HPLC). Affinity of the PCL-ALN particles with HAP was spectrophotometrically confirmed. Antimicrobial activity was quantified by zone of inhibition (ZOI) tests on *S. aureus*. Osteoclast (OC) cultures with PCL-ALN supplements were performed to assess biological responses.

RESULTS: The various emulsion strategies yielded particles with average diameters between 0.80 and 3.05 µm. A high difference in RIF and Gen-AOT encapsulation was observed. The release profiles of RIF showed intense burst release properties while Gen-AOT was released in a sustained way, as was confirmed by plotting the data in a Higuchi graph. PCL particles loaded with Gen-AOT prepared by sonication were chosen for further characterization. The increase of carboxylic acid moieties by surface saponification was established by FTIR analysis and ALN could efficiently be conjugated by EDC/NHS carbodiimide chemistry. Affinity to hydroxyapatite (HAP) of PCL-ALN increased 15-fold, compared with PCL particles (Fig. 1). Drug released from the microparticles could inhibit *S. aureus* for 5 consecutive days. OC cultures confirmed minimal influence of grafted ALN on OC activity.

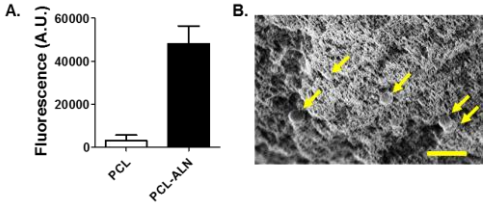

Fig. 1: A) Signal by fluorophore encapsulated in PCL-ALN particles that bound to the scaffold. B) SEM of the scaffold showing the bound particles. (Scalebar = 2 µm)

DISCUSSION & CONCLUSIONS: Due to hydrophilicity of RIF in water (sol_{water} = 1.31 g/L), encapsulation within the PCL particle was low compared to the extremely hydrophobic Gen-AOT. The drugs hydrophobicity and the lower crystallinity of PCL made this formulation prone to the most suitable drug release profile. The 15-fold increase of PCL-ALN bound to the HAP material proofed that these particles experienced chelation of their ALN groups to the calcium in the substrate material. The inhibitory properties against *S. aureus* affirmed the particle`s validity as an antimicrobial drug delivery system. By presenting this bone targeting drug delivery system, we have made the first pre-clinical steps necessary to provide a potential tool for orthopedic surgeons to treat infections of the bone.**ACKNOWLEDGEMENTS:** The authors would like to thank dr. Keith Thompson for his assistance with the cell culture work during this study.

3D Honeycomb patterned fibrinogen based nanofibers induce osteogenic differentiation of mesenchymal stem cells

S. Nedjari[1, 2], D. Gugutkov[2], F. Awaja[2,3], G. Fortunato[1], R. M. Rossi[1], Ge.Altankov[2,4,5]

[1]EMPA Swiss Federal Laboratories for Materials Science and Technology, CH. [2]Institute of Bioengineering of Catalunya, SP. [3]Department of Orthopaedic Surgery, Medical University Innsbruck, AU.[4]Biomedical Research Networking Center in Bioengineering, Biomaterials and Nanomedicine (CIBER-BBN), SP. [5]ICREA (Institucio Catalana de Recerca i Estudis Avançats), SP

INTRODUCTION: Stem cells survival, self-renewal and differentiation are governed by local biochemical and mechanical factors within their niche. The key niche microenvironment includes soluble factors, others cells and extra cellular matrix molecules. While the role of the biochemical signals is extensively studied, the importance of biophysical cues is still not well understood. Electrospinning is a well-established technique to elaborate nanofibers that could mimic the morphology of native extracellular matrix. Therefore, this technique is widely used in tissue engineering. In general, nanofibers are randomly collected but many studies have shown that by controlling the electrostatic forces at the vicinity of the collector, differently patterned nanofibrous scaffolds could be obtained. In this work, we developed a novel composite micropatterned scaffolds. By playing with the electrostatic forces during the electrospinning process, we succeed to manufacture three types of architectures: aligned, honeycomb and random. The composite nanofibers are based on poly (L-lactide ε-caprolactone) PLCL, a biocompatible copolymer, and by fibrinogen (FBG), an important glycoprotein involved in blood coagulation and wound healing.

METHODS: The honeycomb scaffolds were obtained using honeycomb shaped collector produced by photolithography on silicon wafers. The width and the height of the honeycomb walls were 20 and 160 µm. Aligned fibers were obtained using rotating drum during the electrospinning process. To evaluate the biological response of the new electrospun non-wovens, we studied in a comparative manner the attachment (focal adhesions); spreading and the osteogenic differentiation (alkaline phosphatase production, calcification and genes expression) of ADSC Adipose derived mesenchymal stem cells.

RESULTS:

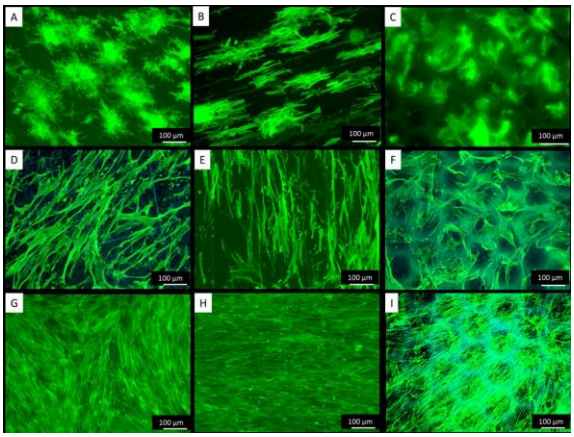

Fig. 1: ADSCs adhering on random (A, D, G), aligned (B, E, and H) and honeycomb (C, F, I) arranged nanofibers. Cells are stained with phalloidin (green) to view actin cytoskeleton after 5 (A-C), day 2 (D-F) and day 6 (G-I) of incubation.

DISCUSSION&CONCLUSIONS:
Morphologically, a clear tendency for an initial cells rounding followed by ADSCs bridging in network was found on honeycomb scaffolds confirming that stem cells recognized the artificial honeycomb niches as 3D micro environment. This supports their homotypic interaction apart from aligned and random scaffolds, where cells are constrained to spread in a rather 2D environment. Honeycomb geometry substantially supports also the osteogenic differentiation of ADSCs confirmed by superior cellular deposition of phosphate and calcium at different incubation period, and qPCR expression of the relevant gene marker of ALP activity and RUNX2 expression.

Artificial tissue cutter: Creation of standardized defects in an osteochondral model

A. Schwab[1], A. Buss[1], S. Naczenski[1], H. Walles[1,2], F. Ehlicke[1]

[1] Tissue Engineering and Regenerative Medicine, University Hospital Würzburg, Würzburg, GER. [2] Fraunhofer ISC Translational Center Würzburg Regenerative Therapies, Würzburg, GER

INTRODUCTION: The treatment strategy to cure cartilage defects is dependent on the lesion severity. Thus, pre-clinical cartilage models need to address clinical relevant defects and geometries ranging from fissures and cartilage only lesions up to osteochondral defects. Aim of this study was the creation of standardized cartilage defects in the *ex vivo* osteochondral model with different depth. Matrix assisted cell free and cell loaded treatment approaches were compared to investigate the influence of defect depth and oxygen tension on cartilage regeneration in *ex vivo* model.

METHODS: Cylindrical Osteochondral explants were isolated from femoral condyle of German landrace pics as described previously. Artificial Tissue Cutter (ARTcut®) is an automated device allowing to wound tissues or biomaterials. Chondral defects (diameter: 4 mm, height: 1 mm) were created with ARTcut® in cartilage of osteochondral explants (diameter: 8 mm). Lesions were left untreated, filled with cell free or chondrocyte loaded collagen I hydrogel (isolated from rat tails) and cultured for 4 weeks under normoxic or hypoxic (5% O_2) conditions. Separated media compartments of custom made culture device allowed for the supply of the explant with tissue specific nutrients: chondrogenic media for cartilage and osteogenic media for subchondral bone without exogenous TGF-β supplementation was used. Live-dead staining was performed to investigate cell viability. Cartilage regeneration was evaluated by (immune) histological stainings as well as quantification of proteoglycan (GAG) content in hydrogels.

RESULTS: Implementation of ARTcut® allowed for creation of standardized chondral defects with a defined depth. With the help of the integrated optical barrier (laser beam) the surface of each sample is approached and set as starting coordinates for drilling the implemented defect depth. Up to 12 explants can be injured at a time.

Live-dead staining did not show evidence of necrotic tissue formation due to drilling. Instead, cell invasion into cell free hydrogel was observed after 4 weeks in live-dead staining originating from surrounding cartilage. Chondrocytes in cell loaded approach synthesized cartilaginous matrix, positive for collagen II and aggrecan. There was a no significant difference in GAG content in cell loaded hydrogel cultured under hypoxic conditions compared to normoxia.

DISCUSSION & CONCLUSIONS: ARTcut® is an innovative wounding device to mimic different cartilage lesion severities and thus study degenerative mechanisms and regenerative treatment strategies *ex vivo*. Comparison of chondral and osteochondral defects allows to study influence of opening subchondral bone on cartilage regeneration in *ex vivo* model. Variation in cell seeding strategies and the combination of different cell types to improve defect repair can also be studied with this model.

ACKNOWLEDGEMENTS: The work leading to these results has received funding from the European Union Seventh Framework Programme (FP7/2007-2013) under grant agreement n° 309962. ARTcut® was developed in cooperation with Fraunhofer ISC (Würzburg).

A tissue adhesive hyaluronan bioink with double gelation mechanism for direct printing into a cartilage defect

D. Petta[1,2], A.R. Armiento[1], D.W. Grijpma[2], M. Alini[1], D. Eglin[1], M. D'Este[1]

[1]AO Research Institute Davos, Davos Platz, Switzerland. [2]Department of Biomaterials Science and Technology, University of Twente, Enschede, The Netherlands

INTRODUCTION: To realize its full potential in tissue engineering and regenerative medicine, 3D bioprinting needs bioinks capable of good extrusion, shape retention, high cell viability and adhesion or integration with native tissues. In this study, we describe a cartilage-adhesive tyramine-modified hyaluronic acid (THA) as a bioink for 3D printing.

METHODS: THA was produced via hyaluronan amidation in water achieving 15.5% substitution degree. THA was dissolved at 2.5% w/v, added to 1) horseradish peroxidase/H_2O_2 for enzymatic crosslinking, and 2) eosin Y (EO) for green light-triggered crosslinking. Rheological properties were measured with an Anton Paar MCR302. Cells laden in the bioink were hMSCs from bone marrow; bovine chondrocytes from fetlock joints and hTERT fibroblasts. Bioprinting was carried out with a RegenHU 3D Discovery® employing a range of pressures and nozzle geometries. Cell viability was assessed with live/dead, CellTiter-Blue® and trypan blue assays in triplicates. Bovine articulations were isolated from stifle joints to print the bioink directly on intact cartilage, full chondral lesions or glass as control; the constructs were washed in PBS to verify the adhesion.

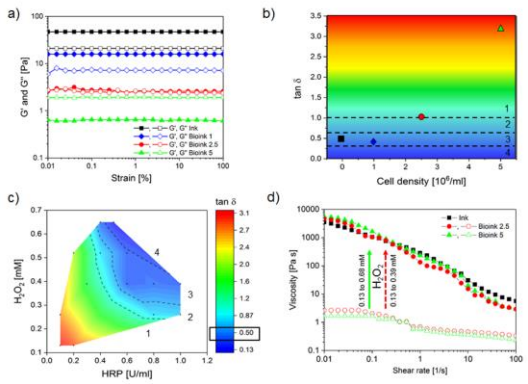

Fig. 1: Viscoelastic properties of the cell-laden enzymatically crosslinked ink. a) Amplitude sweep b) Influence of hMSCs cell density on the tan δ values c) Contour plot showing tan δ d) Flow curves of inks formulation before and after tan δ optimization

RESULTS: THA enzymatic crosslinking produced a soft shear-thinning gel suitable for extrusion and cell encapsulation. Cell addition revealed a dose-dependent decrease in viscoelastic properties which was compensated by increasing H_2O_2 concentration in the precursor (Figure 1). The damping factor was identified as rheologically measurable reliable printability index, with the best results achieved with values between 0.4 - 0.6. Printing at 1 bar with 0.5 mm needles viability up to 93% was achieved. Cell-laden criss-cross constructs with high shape fidelity were printed, displaying 24h viability 78% or above for all cell types (Figure 2). After 14 days culture the viability was maintained or increased. The bioink displayed good adhesion to intact or injured articular surface and was not washed out in wet conditions.

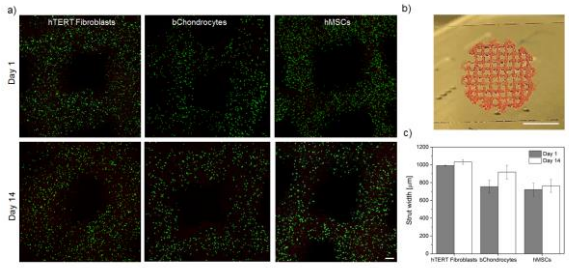

Fig. 2: Viability of cell laden 3D printed constructs with cell density 2.5 x 106 cells/ml. a) Representative L/D images at day 1 and 14 with three embedded cells types, scale bar = 100 µm; b) Macroscopic image of a 3D printed construct, scale bar = 1 cm; c) strut size as function of the embedded cells type at day 1 and 14.

DISCUSSION & CONCLUSIONS: A bioink with good printability, cell viability and adhesion to intact and damaged cartilage tissue was introduced. The double gelation mechanism allowed flexibility and accurate tuning of the bioink and printed structure properties. The damping factor was identified as reliable printability predictor. THA bioink shows the possibility to design bioadhesive bioinks for cartilage tissue engineering in-situ 3D bioprinting.

Design, functionalization and characterization of a bioactive sensing platform to evaluate cell behaviour

G.M. Fortunato[1,2], C. De Maria[1], D. Eglin[2], T. Serra[2], G. Vozzi[1]

[1]Research Centre 'E.Piaggio', University of Pisa, Italy, [2]AO Research Institute, Davos, CH

INTRODUCTION: Conductive polymers (CPs) open new avenues to develop effective strategies for the restoration of damaged or malfunctioning tissues. Biocompatibility, stability over time in biological microenvironment and mild cell-CP interactions should be designed in order to exchange electric signals. The aim of this work is to fabricate and characterize a CP-based substrate to stimulate and evaluate cell response.

METHODS: Conductive substrates were prepared by inkjet printing of 5 up to 50 layers of a conductive ink (Baytron® P, Bayer; PEDOT:PSS 1.3% w/v in H_2O) on a thin cross-linked gelatin substrate. Samples were electrically characterized in dry and wet conditions. A circuit model was obtained through a transfer function fitting of experimental data (impedance analyzer Agilent E4980A). Stability in aqueous environment was also evaluated over a period of 3 weeks in Phosphate-buffered saline. Mechanical characterization was performed by tensile test (Zwick-Roell Z005 ProLine) carried out on samples, evaluating at the same time the dependence of electrical properties on strain rate. Contact angle (Kruss® Drop Shape Analysis System DSA 10), swelling and roughness (FRT^{TM} white light profilometer) of the samples were evaluated.

RESULTS: As schematized in Fig. 1A, a good fitting of the impedance data was a 2-poles and 1-zero transfer function. Impedance measurement of rehydrated samples over 3 weeks showed a good stability (Fig. 1B).

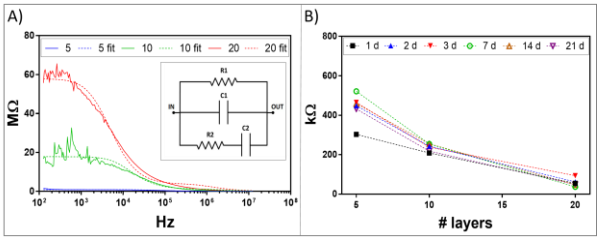

Fig. 1: A) Fitting and circuit model: R1≡PEDOT: PSS - B) R1 values of wet samples over 3 weeks

Tensile test showed that mechanical properties are not influenced by number of PEDOT:PSS layers on the gelatin substrate and impedance is not altered by strain rate. Contact angle measurement highlighted a better hydrophilicity with printed PEDOT:PSS while swelling results showed similar behaviour from 30 min to 14 days of immersion in PBS (Fig. 2).

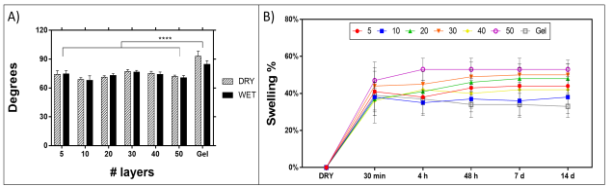

Fig.2: A) Contact angle – B) Swelling test: weight trend

Roughness parameters showed decreasing average roughness (R_a) and mean roughness depth (R_z) as number of printed layers increases.

DISCUSSION & CONCLUSIONS: To evaluate cell response on different samples, myoblast cells (C2C12) will be seeded on top of the samples for 7 days to evaluate metabolic activity and morphology. Based on these overcomes a device for electrical stimulation (Fig. 3) will be developed to evaluate cell alignment, proliferation and differentiation.

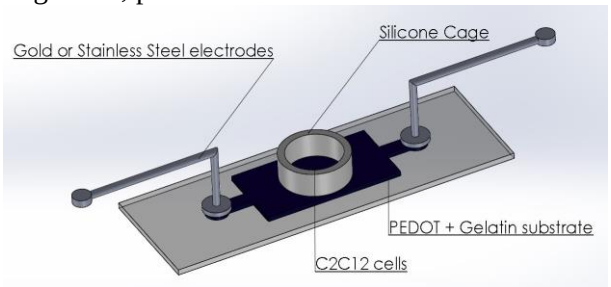

Fig. 3: Concept of the stimulating device

IMPROVED POST-PROCESSING STABILITY OF A 3D PRINTED CEMENT PASTE VIA CO-AXIAL EXTRUSION OF ORGANIC SOLVENTS.

C.M. Sprecher[1], M. Thurner[2], P. Büchler[3], G. Richards[1], D. Eglin[1]

[1] AO Research Institute Davos, Switzerland, [2] regenHU Ltd, Villaz-St-Pierre, Switzerland
[3] Institute for Surgical Technology & Biomechanics and Department of Cranio-Maxillofacial Surgery, Inselspital Bern, University of Bern, Switzerland

INTRODUCTION: 3D printing technology has the potential to allow the manufacturing of truly personalized implants using clinically relevant biomaterials. Calcium phosphate cements are commonly used as synthetic bone fillers and can be amenable to extrusion-based 3D printing. However, extrudable cement pasts have to be flowable enough to be extrudable, but thick enough to conserve their shape upon deposition. In addition, they require post processing for hardening and reaching geometrical stability.
Thus, the goal of the current study was to compare the influence of a conventional extrusion printing with a co-axial extrusion head allowing co-extrusion of the past with organic solvents on the morphology of printed mandibular defect model.

METHODS: With a 3D Discovery™ instrument (regenHU Ltd), a calcium phosphate cement past (OsteoInk™) was printed using a proprietary co-axial printing head, and co-extruded with organic solvents or without (conventional control). For comparison, all printing parameters were kept constant and model structures with an overhang of 72º manufactured. A sterilization cycle at 134ºC was immediately performed post-printing for cement hardening. The morphology of stabilized structures was investigated by X-ray computed tomography (µCT40, Scanco).

RESULTS: The 3D printed calcium phosphate structure stability is improved by using 25 and 50 v:v% ethanol as co-extruded solvents, as shown by the lower angle difference measured in comparison to the CAD design (Table 1). Similar geometry accuracy is achieved as when support structure is printed. Coaxial extrusion with solvents increases the structure porosity in comparison to conventional printing. The structure printed with 50 v:v% Ethanol reaches porosity identical to CAD designed structure. Interestingly, a porosity within the printed calcium phosphate struts is detected by X-ray computed tomography, with an isotropic voxel size of 10 µm, in all samples. A lower amount of porosity is measured in the struts printed in the presence of 25 and 50% Ethanol in comparison to water and conventional printed struts.

DISCUSSION & CONCLUSIONS: 3D printing of a calcium phosphate cement past using a co-axial head and organic solvent has a large influence on the geometric stability and porosity of harden calcium phosphate structures and struts. Using 50% Ethanol as co-extruded solvent, precise replication of planned design porosity which is a prerequisite for accurate and personalized implants was achieved. In addition, medical implants are likely containing complex geometries such as overhangs which with the coaxial head and the 50% Ethanol was reproduced to a precision of less than one degree, averting the need of support structure. From an economical point of view an increased geometry stability reduces the consumption of ink and printing time.
The use of ethanol as solvent seems beneficial for decreasing the porosity in hardened calcium phosphate struts, however the exact mechanisms for the presence and variation of porosity in the hardened calcium phosphate cement need further investigations.

Table 1. Comparison of conventional and co-axial 3D printing.

	Angle difference [degree]	Porosity [%]	
		Structure	Strut
Conventional	10.4±1.7	40.5	3.4±0.9
Water	16.2±8.2	45.7	3.3±1.2
25% Ethanol	0.2±1.3	46.0	1.9±0.6
50% Ethanol	0.5±0.6	60.4	1.4±0.9
CAD design	0	60	
Support structure	0.5		

Development of silk scaffolds with immunomodulatory capacity

A. Zakeri Siavashani[1,2], J. Mohammadi[1], B. Sadeghi[3], B. Senturk[2], M. Rottmar[2], K. Maniura-Weber[2]

[1]*Faculty of New Sciences and Technologies, University of Tehran, Tehran, Iran.*
[2]*Biointerfaces, Empa, Swiss Federal Laboratories for Materials Science and Technology, St.Gallen, CH.* [3]*Department of Laboratory Medicine, Karolinska Institutet, Stockholm, Sweden.*

INTRODUCTION: Implantation of temporary and permanent biomaterials in the body leads to a foreign body reaction (FBR), which may adversely affect the tissue repair process and functional integration of the biomaterial.
To enable a favorable healing response associated with functional tissue formation and improving tissue regeneration, modulation of the inflammatory response is necessary.
This work presents a new immunomodulatory strategy for implanted biomaterials through incorporation of nicotinic acid in 3D pure silk scaffolds as a bone substitute. Nicotinic acid was selected due to its reported potency in modulating the activity of different immune cell types, indicating its promise as an anti-inflammatory drug in the field of biomaterial engineering[2].

METHODS: Silk scaffolds were fabricated by dissolving Bombyx Mori silk fibers in LiBr solution followed by subsequent lyophilization. Nicotinic acid solution with different concentrations of 1, 5, 10 or 12 mM was added drop-wise to silk scaffolds using a micropipette; samples were named as SNP1, SNP5, SNP10, SNP12 and SC (drug-free scaffold). Structural and physicochemical properties of the scaffolds were characterized by scanning electron microscopy, mechanical testing and porosity measurement. Potential cytotoxicity and cell attachment to the scaffolds was evaluated by LDH assay and confocal microscopy using osteoblast-like MG63 cells, respectively.
In vitro immune response to the scaffolds was studied by seeding M1-polarized THP-1 cells (stimulated with LPS and IFN-γ) on the scaffolds with subsequent expression analysis of inflammatory cytokines and markers (TNF-α, CXCL10, CD197a) using ELISA and RT-PCR.

RESULTS: Silk scaffolds showed interconnected porous microstructures and Young modulus of 20.55 ± 1.5 kPa. No toxicity was detected for the nicotinic acid-loaded scaffolds. Moreover, actin/DAPI staining showed good cell attachment and increasing cell number for 7 days of MG63 cell culture. When cultivated on the scaffolds, THP-1-derived M1 macrophages showed a decrease in pro-inflammatory markers at high concentrations of nicotinic acid (Fig1. b-d).

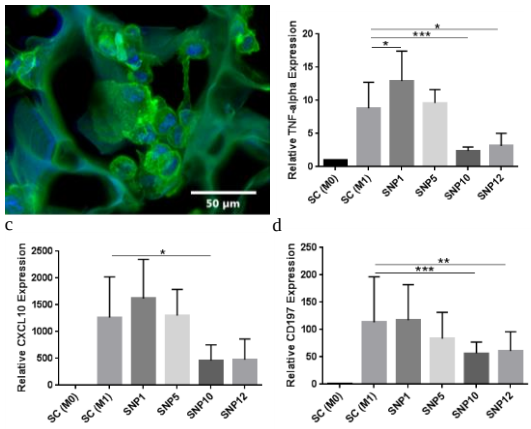

*Fig. 1: Attachment of M1 macrophages to silk scaffolds and relative gene expression of inflammatory factors after 24h. (a) Fluorescent microscopy of M1 macrophages seeded on drug-free scaffold (SC). Relative expression of (b) TNF-α, (c) CXCL10, (d) CD197. Expression levels ±SD were normalized to M0 macrophages seeded on drug-free silk scaffolds. RPL37a was used as a housekeeping gene. n=3 (***p< 0.001, **p< 0.01, *p< 0.05).*

DISCUSSION & CONCLUSIONS: Our data indicate that incorporation of nicotinic acid within silk scaffolds significantly decreases pro-inflammatory cytokines in a concentration dependant manner without any negative effect on the viability and proliferation of MG63 cells.

Degradation of magnesium alloy and bone formation in vivo: micro-CT

Y. Xu[1,2], H. Meng[1], J. Peng[1], S. Lu[1]

[1] Institute of Orthopedics, Chinese P.L.A. General Hospital, Beijing, CN , [2]AO Research Institute Davos, Davos, CH

INTRODUCTION: Magnesium and its alloys have attracted increasing interest as innovative biodegradable materials, particularly due to their potential use as temporary orthopaedic implants. However, uncontrollable degradation limits the application of magnesium alloys, besides, quantitative and non-traumatic in vivo analyses that evaluate the degradation of implants and new bone formation and the association between these two processes are still lacking.

METHODS: 60 micro-arc-oxidized AZ31 magnesium alloy pins (diameter 2.0 mm, length 6.0 mm, weight 0.500 g) were implanted in right femoral condyle of 60 male New Zealand white rabbits. Rabbits were randomly divided into six groups (n=10), and were sacrificed after 1, 4, 12, 24, 36 or 48 weeks (1 group per time-point). Degradation was monitored by weighing the implants prior to and following implantation, and by performing micro-CT scans (images and data were used to assess the degradation of implants and the bone formation) and histological analysis at the six time-points. Experimental values were analysed using an unpaired Student's t-test. $P<0.05$ was indicated a statistically significant difference.

RESULTS: The implants underwent slow degradation in the first 4 weeks, with negligible degradation in the first week, followed by significantly increased degradation during weeks 12-24 ($P<0.05$), and continued degradation until the end of the 48-week experimental period. The magnesium content decreased as the implant degraded, which started at 683.6439 (week 1) and ended at 403.1424 mg/cc (week 48, $P<0.05$); however, the density of the material exhibited almost no change, which ended at 644.9468 mg/cc (week 48). Micro-CT results also demonstrated that pin volume, pin mineral density, mean 'pin thickness', BS/BV and Tb.Sp decreased over time ($P<0.05$), and that the pin surface area/pin volume, BVF, Tb.Th, Tb.N and TMD increased over time ($P<0.05$), indicating that the number of bones and density of new bone increased as magnesium degraded. These support the positive effect of magnesium on osteogenesis. From the maximum inner diameter of the new bone loop and diameter of the pin in the same position, the magnesium alloy was not capable of creating sufficient bridges between the bones and biomaterials when there were pre-existing gaps. Histological analyses showed no inflammatory responses around the implants.

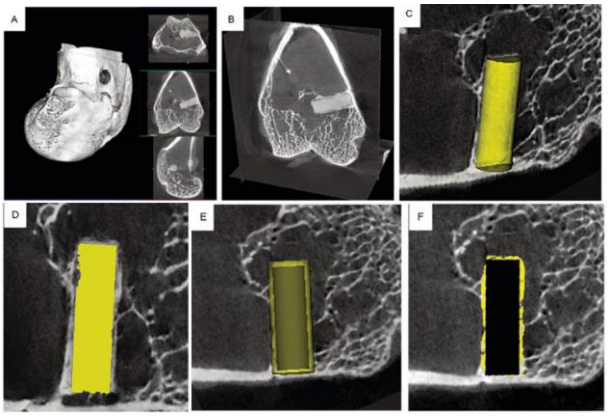

Figure 1: Micro-CT images and 3D reconstruction of the femoral condyle. (A) 3D reconstruction of the femoral condyle and (B) longitudinal section in the 3D coordinate. (C) ROI (diameter=2.0 and length=6.0 mm) and (D) highlight of ROI of the magnesium-alloy pin. (E) New ROI (diameter=2.5 and length=6.5 mm) and (F) highlight of ROI of bone formation around the pin after blanking the previous ROI. ROI, region of interest.

DISCUSSION & CONCLUSIONS: A micro-arc-oxidized AZ31 magnesium alloy is safe in vivo and has a long degradation period. Furthermore, the novel bone formation increased as the implant degraded. The findings concluded that micro-CT, which is useful for providing non-traumatic, in vivo, quantitative and precise data, has great value for exploring the degradation of implants and novel bone formation.

The influence of mechanical stiffness of 3D bioprinted hMSCs-laden scaffolds on cell mineralization, proliferation and differentiation

J. Zhang, J. R. Vetsch, E. Wehrle, M. Rubert and R. Müller

Institute for Biomechanics, ETH Zürich, Leopold-Ruzicka-Weg 4, 8093 Zürich

INTRODUCTION: Understanding how mechanical properties of three dimensional (3D) extracellular matrix influence stem cell differentiation towards the osteogenic lineage is important for bone tissue engineering. However, most studies have focused on two-dimensional (2D) or quasi-3D environments, such as cell seeding on 3D scaffold, which does not represent the real 3D microenvironment *in vivo*. Here we investigate the influence of mechanical stiffness of 3D bioprinted cell-laden scaffolds on human mesenchymal stem cells (hMSCs) proliferation, differentiation towards the osteoblastic/osteocyte lineage and the extracellular matrix mineralization.

METHODS: Two different composite hydrogels with varying amounts of alginate (0.8% and 1.8% w/v) and gelatin (4.09% w/v) were prepared. Bioinks were prepared by mixing hydrogel with hMSCs at a concentration of 5 million cells/ml. 3D cell-laden scaffolds were bioprinted layer-by-layer by the extrusion of the bioink using the INKREDIBLE$^+$ cell bioprinter (CELLINK). In parallel, 3D printed scaffolds without cells served as a negative control. The mechanical properties of the cell-laden scaffolds were characterized by measurement of the compressive moduli at 7 and 14 days of cell culture. In-situ mineralized tissue formation was assessed by weekly micro-computed tomography scans (µCT40, Scanco Medical) within bone bioreactors. DNA content, alkaline phosphatase (ALP) activity, osteogenic-related genes and protein expression were systematically investigated.

RESULTS: Higher alginate concentration resulted in significant higher compressive modulus at day 7. No differences in compressive modulus were observed in the no cells groups at day 7 and day 14 (Fig 1A). However, compressive modulus of cell-laden 0.8%alg significantly increased from 0.66 ± 0.08 kPa at day 7 to 3.7 ± 0.9 kPa at day 14, which was significantly higher compared to no cells 0.8%alg at day 14. Mineral volume increased over time and was significantly higher in the cell-laden 0.8%alg scaffolds (43.5 ± 7.1 mm^3) compared to 1.8%alg scaffolds (22.6 ± 6.0 mm^3) (Fig. 1B). DNA content was significantly higher for 0.8%alg compared to 1.8%alg scaffolds at day 14, 28 and 42 (Fig. 1C). The 0.8%alg scaffolds exhibited a significantly enhanced ALP activity compared to 1.8%alg scaffolds at day 7 and 28 (Fig. 1D). A trend towards higher relative mRNA expression levels of dentin matrix acidic phosphoprotein 1 (Dmp-1, osteocyte marker), was observed in cell-laden 0.8%alg compared to 1.8%alg scaffolds at day 28 and 42 (data not shown). Further, cell-laden 0.8%alg exhibited an osteocyte-like phenotype and had higher collagen I and osteocalcin protein expression than 1.8%alg scaffolds at day 42 (data not shown).

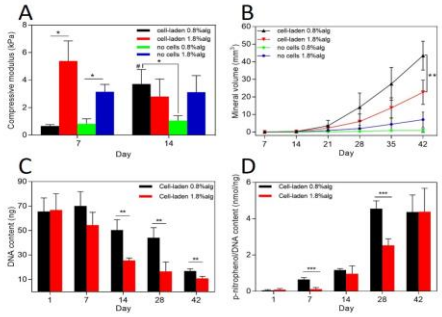

*Fig 1: (A) Compressive modulus, (B) mineral volume, (C) DNA content and (D) ALP activity. * P < 0.05, ** P < 0.01, *** P < 0.005, # P < 0.05 within the same group between day 7 and day 14.*

DISCUSSION & CONCLUSIONS: The results demonstrate that the softer 3D cell-laden 0.8%alg better supports hMSCs differentiation towards the osteocyte lineage, as revealed by higher mineral volume, ALP activity and Dmp1 gene expression. The lower stiffness 3D cell-laden scaffold seems to be promising to promote bone-like tissue formation with potential applications in bone tissue engineering.**ACKNOWLEDGEMENTS:** J. Zhang gratefully acknowledges financial support from CSC.

Optimisation of sacrificial gelatin ink for production of perfusable tubular network in cellularized hydrogel matrix

P. Hatt[1], T. Serra[1], D. Eglin[1]

[1]*AO Research Institute Davos, Davos, CH*

INTRODUCTION: Cellularized matrices with vascular-like network are being developed for understanding and development of therapeutic approaches for damaged or diseased tissues [1]. Among the technologies used to manufacture perfusable tubular network in cellularized hydrogel matrices, such as collagen and fibrin, extrusion-based printing of biocompatible sacrificial template material is an effective method to create complex interconnected and precise porosity. The aim of this work was to optimise the extrusion-based printing of gelatin on hydrogel surfaces, as a sacrificial network generating material for the fabrication of 3D in vitro vascularized model.

METHODS: Gelatin from porcine skin (Fluka) was dissolved in PBS at 5 and 15 w/v % under magnetic stirrer for 2 hrs at 70°C and stored into syringe barrels for 1 hr in the fridge before extrusion-based printing on a 3D Discovery™ (regenHU, Villaz-St-Pierre, Switzerland). Extruded gelatin line diameter (a) (n≥3) was assessed has a function of the gelatin concentration (c), velocity of the printing head (v), needle size (Ø) and pressure (p) while the temperature was kept at 26°C.

RESULTS: A schematic of the envisioned 3D *in vitro* vascularized model bottom-up fabrication process is reported (Fig. 1).

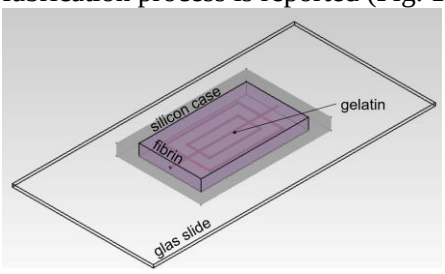

Fig. 1: Schematic illustration of the construct
A silicon case is printed on a glass slide which serves as supporting construct. Secondly, a layer of cellularized fibrin/collagen is casted inside the silicon case. Then, a gelatin network is printed and a second layer of cellularized hydrogel is casted on the top of the network. Finally, the gelatin network is dissolved by flowing warm media through external connection with a perfusion system. Increasing the pressure of printing of gelatin inks leads to an increased line diameter (Fig. 2). Increasing the velocity results in smaller line diameter values. As expected, reducing the needle diameter result in smaller line diameter values and therefore improved circularity for the deposited sacrificial material.

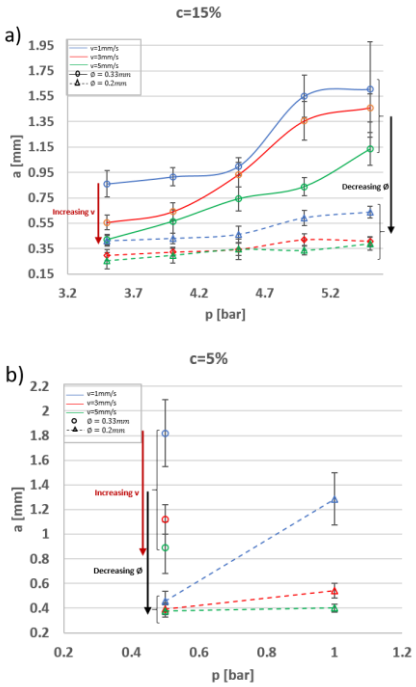

Fig. 2: Influence of p, v, and Ø on line diameter for a) c=15 w/v % and b) c=5 w/v % gelatin sacrificial ink.

DISCUSSION & CONCLUSIONS: 15 w/v % gelatin is a suitable sacrificial ink for the production of high-resolution and reproducible continuous circular struts down to 0.25 mm line diameter. The generation of interconnected perfusable network in fibrin/gelatin hydrogel construct is the next step toward 3D *in vitro* vascularized model.

REFERENCES: [1] P. Datta, B. Ayan, & I. T. Ozbolat (2017) *Bioprinting for Vascular and Vascularized Tissue Biofabrication. Acta biomaterialia*, *51*, 1-20.

Engineering 3D human vascularized models to study cancer cell extravasation

C. Arrigoni[1], M. Crippa[2,3], V. Mainardi[2,3], MV. Colombo[1], S. Bersini[1], M. Gilardi[1], C Candrian[2], M Moretti[1,2,4]

[1]Cell and Tissue Engineering Laboratory, IRCCS Istituto Ortopedico Galeazzi, Milano, IT, [2]Regenerative Medicine Technologies Lab, Ente Ospedaliero Cantonale, Lugano, CH, [3]Department of Chemistry, Materials and Chemical Engineering G. Natta, Politecnico diMilano, IT, [4]Fondazione Cardiocentro Ticino, Lugano (CH)

INTRODUCTION: Investigation of biological mechanisms, e.g cancer metastasis, and discovery of new therapies are hindered by the limitations of current in vitro and in vivo models, which are too simplified or characterized by species-specific differences, respectively. 3D in vitro models have been proposed as a promising tool to overcome these limitations. In this context, we generated vascularized, 3D models both at a microscale and at a meso-scale, replicating the microenvironment of metastatic breast cancer cells (CCs).

METHODS: Microfluidic vascularized models have been generated on the basis of our already developed chips (Fig. 1a), by co-culturing fibroblasts and HUVECs embedded in a fibrin gel. Mesoscale models were also developed based on our previous model, pouring a fibrin gel containing HUVECS and osteoblasts, osteoclasts and macrophages to simulate bone or myoblasts and muscle fibroblasts for muscle tissue in a PMMA mask. In the microfluidic model we investigated the role of platelets and neutrophils in bCCs extravasation. We injected a suspension of bCCs, platelets and neutrophils, treated or not with α2bβ3 integrin inhibitor drug and measured adhesion to HUVECs, extravasation and migration by confocal imaging. In meso-scale models we investigated vascular network development and compared bCCs behavior among bone and muscle.

RESULTS: After 4 days of culture in the chip, HUVECs formed a microvascular network. Injected bCCs were able to adhere to the endothelium, transmigrate through it and invade the matrix. Incubation of bCCs with neutrophils and platelets increased significantly bCCs extravasation whilst the addition of α2bβ3 inhibitor reduced extravasation. α2bβ3 inhibitor increased anti-tumor effects of neutrophils and decreased VE cadherin nuclear translocation in the HUVECs, strengthening HUVECs junctions. In the mesoscale models we obtained a microvascular network, uniformly distributed through the whole 3D tissue at 5 days of culture (Fig 1b). We tested different cell combinations and found that in the bone tissue the microvascular network was more developed as compared to muscle tissue, and even more with the addition of macrophages.

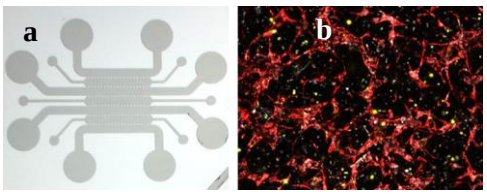

Fig. 1: a) schematics of the channels in the microfluidic chip. b) immunofluorescence of the mesoscale bone model (red HUVECs, white osteoblasts, yellow osteoclasts).

bCCs seeded in the bone and muscle models and to co-localized mainly near the vessels. Furthermore, bCCs growth was significantly decreased in the muscle as compared to the bone model (50% decrease, $p<0.05$).

DISCUSSION & CONCLUSIONS: Micro-and mesoscale models were developed, comprising immune cells, increasingly recognized as key players in the metastatic process. In particular we highlighted the key role of platelets and neutrophils in bCC extravasation. Furthermore, we showed that inhibition of α2bβ3 integrin decreased bCCs extravasation through different biological mechanisms, strengthening the previous findings of anti-metastatic effects of an approved drug. On the other hand, vascularized mesoscale models of bone and muscle tissue were generated, showing the possibility to mimic organ-specific bCCs proliferation. The study of bCC behaviour in these complex models, which better reproduce in vivo milieu as compared to standard ones, can help to identify new mechanisms underlying metastatic processes in a more reliable way.

The best of both worlds: using minced pieces of autologous cartilage as a chondrocyte source combined with a bioactive scaffold for cartilage repair applications

D. Mostafa sindi[1], C. Levinson[1], E. Cavalli[1], G. M. Salzmann[2], P. Neidenbach[2], M. Zenobi-Wong[1]

[1] Tissue Engineering + Biofabrication, ETH Zürich, Zürich, Switzerland, [2] Schulthess Clinic, Musculoskeletal Centre, Orthopaedics Lower Extremities, Zurich, Switzerland

INTRODUCTION: Autologous chondrocyte implantation (ACI) represents the gold standard among currently available techniques for articular cartilage repair. ACI, however, is a two-step surgical procedure and requires *ex vivo* cell expansion, which is complex and expensive. A second-generation autologous minced cartilage repair technique was developed to deliver chondrocytes in a one-step surgery without cell expansion. This technique relies on mechanical fragmentation of cartilage tissue to provide an increased surface area for chondrocytes to outgrow. Minced cartilage pieces are fixed into defect site using fibrin glue adhesive. The aim of this study was to improve this technique by evaluating Collplant, a soft tissue matrix consisting of human recombinant collagen and autologous PRP, as a fibrin glue substitute. Furthermore, the potential of a custom-made device (prototyped by Arthrex) to provide a faster and easier way to mince cartilage was tested.

METHODS: Human cartilage samples from total joint replacement patients were prepared and minced either by hand or by the Arthrex device into small fragments (~1 mm^3), embedded in either fibrin glue or Collplant and cultured for up to 4 weeks. The viability of chondrocytes in hand-minced and device-minced cartilage pieces at day 0 and day 7 was assessed. Furthermore, the viability of chondrocytes embedded in fibrin glue and Collplant, and their ability to outgrow and produce cartilage-specific matrix were assessed at day 28.

RESULTS: The effect of Collplant on chondrocyte viability, outgrowth, and matrix deposition was evaluated and compared to fibrin glue adhesive. The performance of the mincing device was evaluated and compared to hand mincing. After a significantly lower initial viability, device-minced cartilage pieces embedded in both fibrin glue and Collplant revealed comparable viability and outgrowth potential to hand-minced groups. Matrix deposition as visualized by Safranin O and collagen I/II staining exhibited only negligible staining for all groups.

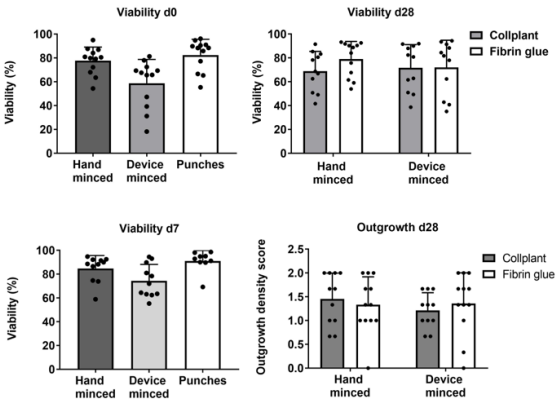

Fig. 1: The viability of chondrocytes in hand- and device-minced cartilage pieces was assessed at day 0 and day of culture. The viability of chondrocytes embedded in fibrin glue and Collplant was assessed at day 28 of culture. The ability of chondrocytes to outgrow from cartilage pieces embedded in either fibrin glue or Collplant was evaluated using a scoring scheme: 0 = no outgrowth, 1 = moderate outgrowth and 2 = high number of outgrown cells.

DISCUSSION & CONCLUSIONS: This study suggests that Collplant and the prototype device possessed comparable performance to fibrin glue and hand mincing respectively. The results support the great potential of Collplant and prototype device for their use in second-generation autologous minced cartilage repair techniques.

ACKNOWLEDGEMENTS: The authors thank Arthrex Swiss AG for providing the prototype of the mincing device.

3-D bioprinting of a human omentum model: Mimicking the mesothelial cell layer and microenvironment *in vivo*

M. Estermann, D. Septiadi, A. Petri-Fink, B. Rothen-Rutishauser

Adolphe Merkle Institute, University of Fribourg, Switzerland

INTRODUCTION: Women diagnosed with ovarian cancer often have a low survival rate as they show already peritoneal dissemination involving the greater omentum as major site of metastasis. To obtain a better understanding of the ovarian cancer spreading in the greater omentum, *in vitro* models investigating cell adhesion and invasion were recently established. However, these models do not fully represent the *in vivo* omental microenvironment as representative cell types were lacking and the tissue specific structure was not considered. Hence, a reliable *in vitro* model mimicking the specific structure of the human omentum is required. Three dimensional (3-D) bioprinting technology has recently advanced providing a promising approach to establish reproducible *in vitro* models. Bioprinting allows a spatially controlled deposition of cells and biomaterials and offers a useful tool to address tissue specific structures. In the following project, we aim to bioprint a human omentum cancer model consisting of several cell types and biomaterials acting as bioinks. A close imitation of the cell morphology and microenvironment is aimed. First results of a bioprinted the mesothelial cell layer are reported.

METHODS: The human mesothelial cell line MeT-5A was printed on collagen type I coated inserts using the 3D Discovery™ from regenHU. Printing parameters and pattern were optimized to obtain a homogeneous collagen coating and cell distribution. As a close imitation of the mesothelial cell layer in situ is aimed, cell morphology and the microenvironment of the chosen cell line were evaluated. Mesothelial cells of the human omentum express microvilli and therefore the morphology and surface functionalization of the MeT-5A cells cultured for 10 days was investigated using scanning electron microscopy (SEM). The optimal microenvironment of this cell line was assessed using different combinations of extracellular matrix (ECM) proteins. The degree of cell attachment was evaluated quantitatively after 48 hours in culture.

RESULTS: SEM imaging showed that the MeT-5A cells expressed microvilli ranging from 1 – 2 µm when cultured for 10 days. The quantitative analysis of different combinations of ECM proteins could reveal that the combination of collagen type I and fibronectin resulted in the highest cell attachment.

DISCUSSION & CONCLUSIONS: The aim of the performed experiments was to evaluate the capability to imitate the *in vivo* mesothelial cell layer regarding morphology and microenvironment. MeT-5A formed microvilli when bioprinted on collagen type I allowing a close imitation of the *in vivo* cell morphology. In addition, the ECM protein composition resulting in the highest cell attachment is similar to the ECM of the submesothelium of the human omentum, which is composed of collagen type I, fibronectin and vitronectin[3]. We can conclude that both cell morphology and ECM protein composition resembles closely the *in vivo* mesothelial cell layer and microenvironment providing a promising approach to establish a realistic *in vitro* model. Further work will include the consideration the tissue specific structure and the investigation of ovarian cancer cell adhesion and invasion.

ACKNOWLEDGEMENTS: This project is supported by the Sinergia grant "The underestimated role of the human omentum in metastatic spread" from the Swiss National Science Foundation (Nr. CRSII5_171037 / 1). In addition, we would like to thank Dr. Ching-Yeu Liang and Dr. Francis Jacob from the University Hospital in Basel and Dr. Ana Bela Torres from FHNW for their support.